

Examination of the Superconductor $\text{Hg}_{1-x}\text{Zn}_x\text{Ba}_{1.5}\text{Sr}_{0.5}\text{Ca}_2\text{Cu}_3\text{O}_{8+\delta}$ Structural and Electrical Properties

Kareem A. Jasim ^{1,a)}, Nabaa Safaa Hamzah ^{1,b)}, Marwa Mohammed Ahmed ^{1,c)} and Mudatheer M. Al-Slivani ^{2,d)}

¹ Department of Physics, College of Education for Pure Sciences, Ibn Al-Haitham, University of Baghdad, Iraq.

² Department of Physics, College of Education for Pure Sciences, University of Al-Furqan, Mosul, Iraq.

^{a)} kareem.a.j@ihcoedu.uobaghdad.edu.iq

^{b)} nabaa.s.h@ihcoedu.uobaghdad.edu.iq

^{c)} marwa.m.a@ihcoedu.uobaghdad.edu.iq

^{d)} corresponding author: mudatheeralslivani@gmail.com

Abstract. This study investigates the effect of partial Zinc (Zn) substitution for Mercury (Hg) on the structural, morphological, and electrical properties of the $\text{Hg}_{1-x}\text{Zn}_x\text{Ba}_{1.5}\text{Sr}_{0.5}\text{Ca}_2\text{Cu}_3\text{O}_{8+\delta}$ (Hg-1223) high-temperature superconducting system. Polycrystalline samples with Zn concentrations of $x = 0, 0.05$, and 0.15 were prepared via the solid-state reaction method under specific sintering and pressure conditions. The structural characterization was performed using X-ray diffraction (XRD), while surface morphology was analyzed by Scanning Electron Microscopy (SEM). Electrical properties were determined through resistivity measurements using the standard four-probe method. XRD analysis confirmed that all samples possessed a tetragonal crystal structure, with Zn substitution enhancing the crystallinity and increasing the 'c' lattice parameter. SEM micrographs showed that Zn doping promoted significant grain growth, resulting in a denser, more compact, and better-interconnected microstructure compared to the pure sample. Most notably, the superconducting properties were significantly enhanced with Zn substitution. The zero-resistance critical temperature ($T_c(\text{offset})$) increased from 105 K for the undoped sample ($x=0$) to a maximum of 123 K for $x=0.15$. This enhancement was accompanied by a narrowing of the superconducting transition width (ΔT_c) from 23 K to 9 K. This atypical increase in T_c upon substitution is attributed to the improved structural regularity and grain connectivity, and a 'c'-axis expansion potentially optimizing the hole carrier concentration.

Keywords: Sintered Temperatures, Pressure, Critical Temperature, Four-Probe Method and Scanning Electron Microscopy

INTRODUCTION

Superconductivity, which is the ability of some metals, alloys, and types of ceramics to transfer electric current without resistance at low temperatures, is one of the phenomena that altered the study of materials[1]. The Dutch scientist Kimberling Onnes discovered superconductivity in 1911 while attempting to determine whether the specific resistance of metals at very low temperatures would follow a linear decrease with a decrease in temperature or if would it hold at a specific value. Mercury's resistance abruptly vanishes (i.e., approaches zero, or 4.2 K) when it is cooled with liquid helium, according to an analysis of mercury resistance as a function of temperature. This process is referred to as superconductivity. The temperature at which a substance changes from its normal state to superconductivity is called a critical temperature or transition temperature (T_c) for the state of superconductivity, and this value varies from one substance to another [2]. The first phase of the series $\text{HgBa}_2\text{Ca}_{n-1}\text{CuO}_{2n+2+\delta}$, with a critical temperature of 94 K and the structural formula $\text{HgBa}_2\text{CuO}_{4+\delta}$, was discovered by Putilin et al. in 1993 [3].

After that, in the same year, Schilling et al. found that the Hg-Ba-Ca-Cu-O system, which has the structural formula $\text{HgBa}_2\text{Ca}_2\text{Cu}_3\text{O}_{8+\delta}$, had a critical temperature of 133 K. Later, Schilling et al. found that the critical temperature in the superconducting system (Hg-1223) climbs to 164 K at a pressure of 105 Pa depending on the mercury series $\text{HgBa}_2\text{Ca}_{n-1}\text{CuO}_{2n+2+\delta}$, (Hg-1245 and Hg-1234, Hg-1212) [4]. Mercury-based superconductors have layers of copper oxide that superconduct copper oxide layers, dielectric layers that can behave as the hole's electron-active charge stores, and layers of copper and oxygen that donate electrons to the crystal structure [5-8]. The CuO layers can be considered to be derived from the perovskite structure by removing oxygen overlap from among CuO layers, while the dielectric layer is derived from the rock salt structure. To improve some superconducting properties and raise the critical temperature, the researchers performed the compensatory or partial replacement of some

elements of the superconducting compounds with other elements by partial replacement and improved the superconducting properties [9–14]. The phase formation of Hg-1223 and critical current density can be improved by partially replacing some upper valence elements, such as Sr, Pb, Y, or others. In this paper, we will prepare three samples of $\text{Hg}_{1-x}\text{Zn}_x\text{Ba}_{1.5}\text{Sr}_{0.5}\text{Ca}_2\text{Cu}_3\text{O}_{8+\delta}$ superconductivity with $x = 0, 0.05$, and 0.15 using the solid-state reaction method and with different preparation conditions. And analyze the structural and electrical properties, and study the effect of partial replacement of Zn with mercury on the critical temperature increase at zero resistance $T_{c(\text{offset})}$ and starting resistance $T_{c(\text{onset})}$.

EXPERIMENTAL PART

A Shimadzu X-ray machine, configured with a Cu $K\alpha$ source (wavelength 1.5406) operating at 40 kV and 30 mA, was employed to examine the structural properties of the samples. The purpose was to acquire data for diagnosing the phases formed within the samples, along with their proportions, by analyzing 2θ , d , and hkl values. The X-ray diagram, in conjunction with computational programs [16, 17] and the application of Bracken's law of deviation, was used to calculate the lattice constants a , b , and c , as well as the network coefficients per unit cell. The structural characteristics of the compound were investigated via X-ray diffraction analysis, specifically focusing on samples prepared at an annealing temperature of 850°C and under a pressure of 8 tons per cubic meter. This XRD study of samples with different x ratios indicated that the $x = 0$ sample displayed a regular crystalline structure, evident from the clear peaks shown in Figure 1. By utilizing Bragg's law of diffraction, the values for d_{hkl} (the distance between parallel planes) were determined. Following the determination of Miller coefficients (hkl), the lattice parameters a , b , and c were computed from the reflection angles using a computer program based on the Full Prof Suite [18, 19].

RESULTS AND DISCUSSION

In the present study, all the samples were characterized using X-ray diffraction to determine the gross structural characteristics. Representative XRD patterns are shown in Figure 1. All the XRD data of different samples (with different concentrations of Hg, Ba, Sr Ca, Cu and Zn) were polycrystalline and corresponded to Hg (Zn)-1223 phases. Also, XRD demonstrates the presence of a small number of impurities phases at infinitely small levels. In the samples of all Hg-base systems, it is possible to see it through the spectra that there are two main phases: high T_c (1223) and low T_c (1212) and several impurity phases of $(\text{Ca}, \text{Ba}, \text{Sr})_2\text{CuO}_3$, CaZnO_4 and CuO . Problems in stacking along the c -axis may be associated with the emergence of more than two phases. Comparison of relative XRD patterns intensities of samples with $\text{Zn} = 0.05$ and 0.15 with relative intensities of same reflections of sample with $\text{Zn} = 0.0$ indicate that all the samples have reflection intensities of high T_c phase reflections (H), reflection intensities of low T_c phase reflections (L). As the mass of Zn increased, the low- T phase became larger, H peaks became smaller, and low T_c became smaller.

The free sample's ($\text{Zn} = 0$) High- T_c phase reflections are less intense than the Zn-containing samples. The lattice parameters were calculated using the d data values and reflectance (hkl) of the observed X-ray diffraction pattern by a Cohen-based software, the least square method [20, 21], parameters a , b , c , mass density M , and volume fraction (V_{phase}) shown in Table 1. It was found that the lattice parameters for all samples are $a = b \neq c$, meaning that it is of the Tetragonal structure [22-25]. It was observed that the diffraction peaks became more defined, characterized by narrower bases, as the compensation ratio for x was adjusted to 0.15 . This development signifies an enhanced crystalline structure (or crystallinity) and is accompanied by an increase in peak intensity. Furthermore, the d_{hkl} values, which represent the separation between parallel planes, were computed using Bragg's law of diffraction. The Miller coefficients (hkl) were identified from the 2θ angles of reflection, and the results were subsequently processed using the software-based Cohen's least squares method. Also, it was found that the model maintains the type (Tetragonal), but it showed an increase in the dimension (c), which indicates an increase in the regularity in the crystalline structure, and the values of lattice parameters at $x = 0$ are $a = b = 3.74 (\text{\AA})$, $c = 15.69 (\text{\AA})$. It was also found that increasing the compensation ratio to 0.2 showed an increase in the x values and their regularity with an increase in lattice parameters (a , b , c), they became $a = b = 3.75 (\text{\AA})$ and $c = 15.79 (\text{\AA})$, as we noticed a regularity in the composition as shown in Table 1. The crystal structure of the compound changes when the compensation ratio is increased and the compound becomes a better crystalline structure [18,19]. As shown in Table 1, the mass density (M) values increased with the addition of the Zn element, while the volume fraction (V_{phase}) values decreased when the Zn concentration increased from 0.05 to 0.15 . These results are consistent with the results obtained by the researchers in references [22, 26].

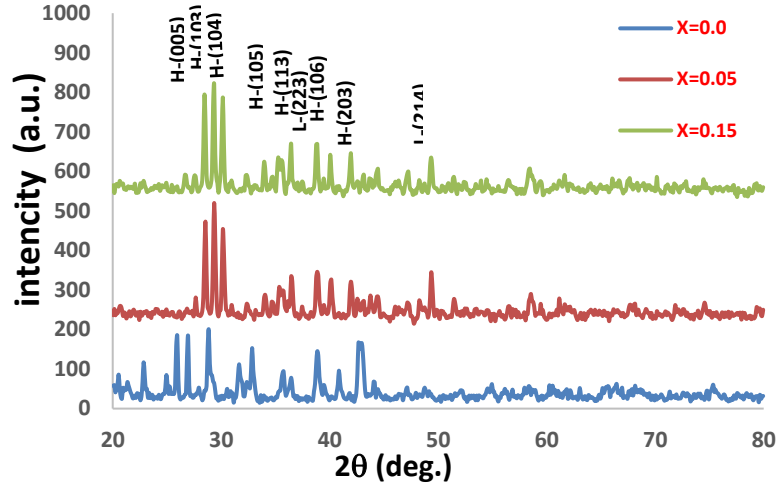


FIGURE 1. X-ray diffraction showing $\text{Hg}_{1-x}\text{Zn}_x\text{Ba}_{1.5}\text{Sr}_{0.5}\text{Ca}_2\text{Cu}_3\text{O}_{8+\delta}$ for the specified values with $\text{Zn} = 0, 0.05$ and 0.15 "

As an indication of temperature. It is noted from Figure 2 and Table 1 that the $\text{Hg}_{1-x}\text{Zn}_x\text{Ba}_{1.5}\text{Sr}_{0.5}\text{Ca}_2\text{Cu}_3\text{O}_{8+\delta}$ superconductor with $x = 0$, sample possesses an initial transition temperature ($T_{c(\text{onset})}$) close to 128 K and the zero value $T_{c(\text{offset})}$ was 105 K, while the initial transition temperature approached 134 K and the zero value was 115 K as adding small amounts of $\text{Zn} = 0.05$. But when the Zink is increased to 0.15 the initial increase 132 K and zero transition temperatures increase to 123 K with the increase of Zink, as shown in Table 1. The width of the transition temperature changed when the Zink concentration increased from 0 to 0.15 (the difference between the initial and zero) as follows: 23, 19, 8, and 9, respectively, as shown in Table 1.

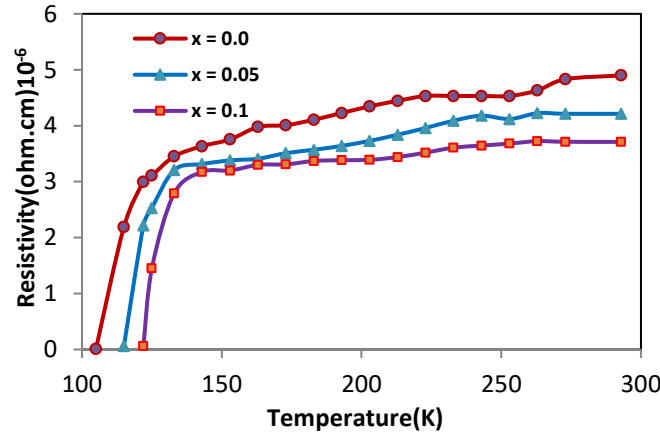


FIGURE 2. Resistivity dependence of temperature for $\text{Hg}_{1-x}\text{Zn}_x\text{Ba}_{1.5}\text{Sr}_{0.5}\text{Ca}_2\text{Cu}_3\text{O}_{8+\delta}$ at the specified Zn values " $x = 0.0, 0.05$ and 0.1 ".

TABLE 1. Values of transition temperature $T_{c(\text{offset})}$, $T_{c(\text{onset})}$ and ΔT_c and lattice at the specified Zn values " $x = 0, 0.05$ and 0.1 "

<i>Zn Partial Substitution</i>	<i>$T_{c(\text{onset})}$ (K)</i>	<i>$T_{c(\text{offset})}$ (K)</i>	<i>ΔT (K)</i>
0	128	105	23
0.05	134	115	19
0.15	132	123	9

Scanning electron microscopy (SEM) techniques were used to analyze the surface morphology, grain size, and interconnectivity of the prepared samples [27]. Microstructure is a crucial factor that directly affects superstructure properties, as it can be influenced by factors such as sintering temperature and impurity concentration. SEM images

showed a clear evolution in grain shape with increasing zinc (Zn) concentration [19]. In the pure sample ($x=0$), the grains were relatively smaller and less interconnected, with clear porosity (gaps) between the grains. With increasing Zn concentration (up to $x=0.15$), the images show a significant and marked improvement in microstructure. The grains became noticeably larger, more compact, and denser. This indicates that the zinc substitution acted as a sintering aid, promoting grain growth and improving the packing fracture between them.

The importance of this increased interconnectivity is that the grains minimize the number of weak links which are resistive boundaries between grains. It is this enhancement in microstructure that offers a direct scientific explanation of the enhancement in the superconducting properties. The bigger and closer packed grains provide a more robust and long-term conductive route of superconducting current, which best fits the high critical temperature ($T_c(\text{offset})$) and small superconducting time found in the sample $x=0.15$. Moreover, it was possible to identify the various phases based on the microscopic image analysis and X-ray diffraction data [29]. The major phase Hg-1212 (white contrast) was seen to be present, and the minor phases were zinc-free phases (dark gray), Hg-2212 (gray contrast) and zinc-rich regions (light gray). Certain traces of interfaces growth of the Hg-1223 phase inside Hg-1212 grains were also detected [28], this could help to improve the stability of the said conductors and help provide them with better attributes.

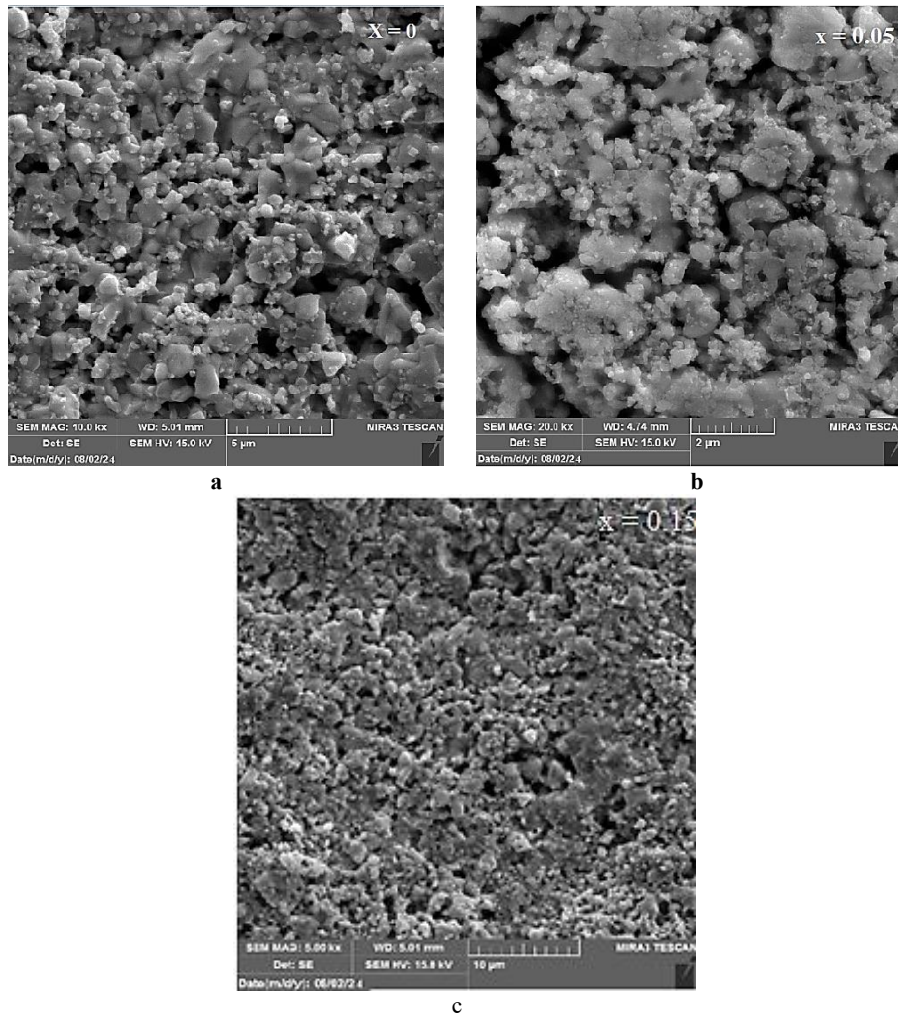


FIGURE 3a,b,c. Scanning electron microscope images obtained on smooth, polished samples. For $\text{Hg}_{1-x}\text{Zn}_x\text{Ba}_{1.5}\text{Sr}_{0.5}\text{Ca}_2\text{Cu}_3\text{O}_{8+\delta}$ compound samples at the specified values $\text{Zn} = 0, 0.05$ and 0.15 .

The fact that $T_c(\text{offset})$ changes with Zn substitution is an important observation. The replacement of cations in superconductors usually destabilizes the structure and discourages T_c . Possibly, however, the reason is our XRD data. We see an increase in the crystalline structure and the regularity of the composition increases. This is

associated with the enlargement of the lattice constant 'c'. This expansion of the c-axis is interesting, because Zn^{+2} has a smaller ionic radius than Hg^{+2} . This implies that substitution mechanism is not straightforward. The increased regularity in structure and lattice expansion can favor the spacing between the CuO_2 planes or, more probably, modify the oxygen quantity in the HgO delivery layer of the HgO ions. This structural modification might maximize the concentration of the hole carriers in the CuO_2 planes to bring the system to the highest possible T_c and, therefore, justify the observed improvement.

CONCLUSIONS

In this investigation, the structural, morphological, and electrical properties of the high-temperature superconducting system $\text{Hg}_{1-x}\text{Zn}_x\text{Ba}_{1.5}\text{Sr}_{0.5}\text{Ca}_2\text{Cu}_3\text{O}_{8+\delta}$, with zinc concentrations of $x = 0, 0.05$, and 0.15 , were systematically examined. Polycrystalline samples were successfully synthesized via the solid-state reaction method. The study confirms that partial substitution of mercury with zinc exerts a significant and beneficial influence on the superconducting characteristics of the Hg-1223 phase. The X-ray diffraction structural analysis revealed that all the prepared samples possessed the tetragonal crystal structure. The next important effect of the substitution of zinc was the upsurge in the crystallinity of the material whereby the diffraction peaks were sharper and stronger, particularly the ones in the sample of $x = 0.15$. Moreover, the replacement led to an increase in c lattice parameter. Such augmentation in c-axis in spite of a reduced ionic radius of Zn in comparison with Hg suggests a complex substitution course that is likely to modify the oxygen content (d) of the layer of charge reservoir and consequently maximize the concentration of hole carriers. The SEM scan revealed that there was a high surface morphology increase. The grains were reduced and the unpatched sample was quite porous. On the other hand, zinc replacement contained effective sintering aid, and this increased high growth of the grain. This provided a much closer-packed, smaller and more interconnected microstructure. This improved contact of the grains is relevant, since it will reduce the occurrence of weak links at the interfaces of the grains so that solid path of the superconducting current flow could be achieved more frequently. The greatest outcome of the research is that the superconducting properties are increased considerably. The critical temperature (T_c (offset)) was found to rise significantly with x (105 K in the pure sample ($x=0$)) reaching a maximum critical temperature of 123 K in the $x=0.15$ sample. At the same time, the superconducting transition width (ΔT_c) was narrowed significantly, 23 K was reduced to 9 K. Such sharpening of the transition means that the homogeneity of the superconducting phase has significantly increased. This unusual increase in T_c with substitution can be directly related to the effect of increased structural regularity and enhancement of microstructural integrity, i.e., the increased grain growth and interconnectivity, to the advantage of the zinc doping.

REFERENCES

1. M. A. Mudatheer, M. A. Hammod, and M. A. Abed, "Impact of Zn and Sr substitution on the structural, electrical, and insulating properties of Bi-based high-temperature superconductors prepared via solid-state reaction and double annealing process," *J. Mater. Sci. Mater. Electron.*, vol. 36, no. 5, pp. 1885–1895, 2025, doi: 10.1007/s10854-025-15887-5.
2. M. A. Mudatheer, M. A. Hammod, and M. A. Abed, "Double partial substitution effect of Zink (Zn) and strontium (Sr) on the structural and electrical properties of high-temperature $\text{Bi}_{2-x}\text{Zn}_x\text{Ba}_{2-y}\text{Sr}_y\text{Ca}_2\text{Cu}_3\text{O}_{10+\delta}$ superconductor," *Funct. Mater.*, vol. 32, no. 1, pp. 42–49, 2025, doi: 10.15407/fm32.01.42
3. S. Putlin, E. Antipov, and M. Marezio, "Superconductivity above 120 K in $\text{HgBa}_2\text{CaCu}_2\text{O}_{6+\delta}$," *Physica C: Superconductivity*, vol. 212, no. 3-4, pp. 266-270, 1993, doi: 10.1016/0921-4534(93)90588-h.
4. A. Schilling, M. Cantoni, O. Jeandupeux, J. D. Guo, and H. R. Ott, "Physical and structural aspects of the 130 K superconductor in the Hg-BA-Ca-Cu-O system," *Advances in Superconductivity VI*, pp. 231-236, 1994, doi: 10.1007/978-4-431-68266-0_48.
5. B. A. Omar, S. J. Fathi, and K. A. Jassim, "Effect of Zn on the structural and electrical properties of high-temperature $\text{HgBa}_2\text{Ca}_2\text{Cu}_3\text{O}_{8+\delta}$ superconductor," *AIP Conference Proceedings*, vol. 1968, p. 030047, 2018.
6. K. A. Jasim, S. A. Makki, and A. A. Almohsin, "Comparison study of transition temperature between the superconducting compounds $\text{Tl}_{0.9}\text{Pb}_{0.1}\text{Ba}_2\text{Ca}_2\text{Cu}_3\text{O}_9$, $\text{Tl}_{0.9}\text{Sb}_{0.1}\text{Ba}_2\text{Ca}_2\text{Cu}_3\text{O}_{9-\delta}$ and $\text{Tl}_{0.9}\text{Cr}_{0.1}\text{Ba}_2\text{Ca}_2\text{Cu}_3\text{O}_{9-\delta}$," *Physics Procedia*, vol. 55, pp. 336–341, 2014.

7. H. M. J. Haider, K. M. Wadi, H. A. Mahdi, K. A. Jasim, A. H. Shaban, "Studying the partial substitution of barium with cadmium oxide and its effect on the electrical and structural properties of $\text{HgBa}_2\text{Ca}_2\text{Cu}_3\text{O}_{8+\delta}$ superconducting compound," AIP Conference Proceedings, vol. 2123, p. 020033, 2019, doi: 10.1063/1.5116960.
8. L. Gao, Z. Huang, R. Meng, J. Lin, F. Chen, L. Beauvais, Y. Sun, Y. Xue, and C. Chu, "Study of superconductivity in the Hg-Ba-Ca-Cu-O system," Physica C: Superconductivity, vol. 213, no. 3-4, pp. 261-265, 1993, doi: 10.1016/0921-4534(93)90440-2.
9. A. Schilling, M. Cantoni, J. D. Guo, and H. R. Ott, "Superconductivity above 130 K in the Hg-Ba-Ca-Cu-O system," Nature, vol. 363, no. 6424, pp. 56-58, 1993, doi: 10.1038/363056a0.
10. A. K. Saadon, A. H. Shaban, K. A. Jasim, "Effects of the Ferrits addition on the properties of Polyethylene Terephthalate," BZn hdad Science Journal, vol. 19, no. 1, pp. 208–216, 2022.
11. P. Sastry, Y. Li, J. Su, and J. Schwartz, "Attempts to fabricate thick HgPb_{1223} superconducting films on Zink," Physica C: Superconductivity, vol. 335, no. 1-4, pp. 112-119, 2000, doi: 10.1016/s021-4534(00)00154-4.
12. A. N. Abdulateef, A. Alsudani, R. K. Chillab, K. A. Jasim, and A. H. Shaban, "Journal of Green Engineering," vol. 10, no. 9, pp. 5487–5503, 2020.
13. R. S. A. Al-Khafaji and K. A. Jasim, "Dependence of the microstructure specifications of earth metal lanthanum La substituted $\text{Bi}_2\text{Ba}_2\text{CaCu}_2\text{-XLaXO}_{8+\delta}$ on cation vacancies," AIMS Materials Science, vol. 8, no. 4, pp. 550–559, 2021.
14. E. Engler, R. Beyers, V. Lee, A. Nazzal, G. Lim, S. Parkin, P. Grant, J. Vazquez, M. Ramirez, and R. Jacowitz, "Processing, structure, and high-temperature superconductivity," International Journal of Modern Physics B, vol. 1, no. 2, pp. 189-194, 1987, doi: 10.1142/s0217979287000153.
15. R. Costa, A. Jurelo, P. Rodrigues, P. Pureur, J. Schaf, J. Kunzler, L. Ghivelder, J. Campá, and I. Rasines, "Splitting of the bulk resistive transition in high- T_c superconductors: Evidence for unconventional pairing," Physica C: Superconductivity, vol. 251, no. 1-2, pp. 175-182, 1995, doi: 10.1016/0921-4534(95)00399-1.
16. K. A. Jasim and T. J. Alwan, "Effect of Oxygen Treatment on the Structural and Electrical Properties of $\text{Tl}_{0.85}\text{Cd}_{0.15}\text{Sr}_2\text{CuO}_{5-\delta}$, $\text{Tl}_{0.85}\text{Cd}_{0.15}\text{Sr}_2\text{Ca}_2\text{Cu}_2\text{O}_{7-\delta}$ and $\text{Tl}_{0.85}\text{Cd}_{0.15}\text{Sr}_3\text{Ca}_2\text{Cu}_3\text{O}_{9-\delta}$ Superconductors," Journal of Superconductivity and Novel MZn netism, vol. 30, no. 12, pp. 3451–3457, 2017.
17. K. A. Jasim, "The effect of cadmium substitution on the superconducting properties of $\text{Tl}_{1-x}\text{Cd}_x\text{Ba}_2\text{Ca}_2\text{Cu}_3\text{O}_{9-\delta}$ compound," Journal of Superconductivity and Novel MZn netism, vol. 26, no. 3, pp. 549–552, 2013.
18. S. H. Aleabi, A. W. Watan, E. M.-T. Salman, K. A. Jasim, A. H. Shaban, and T. M. Alsaadi, "The study effect of weight fraction on thermal and electrical conductivity for unsaturated polyester composite alone and hybrid," AIP Conference Proceedings, vol. 1968, p. 020019, 2018.
19. K. A. Jasim, "Superconducting properties of $\text{Hg}_{0.8}\text{Cu}_{0.15}\text{Sb}_{0.05}\text{Ba}_2\text{Ca}_2\text{Cu}_3\text{O}_{8+\delta}$ ceramic with controlling sintering conditions," Journal of Superconductivity and Novel MZn netism, vol. 25, no. 6, pp. 1713-1717, 2012, doi: 10.1007/s10948-012-1507-3.
20. B. A. Ahmed, J. S. Mohammed, R. N. Fadhil, A. H. Shaban, and A. H. Al Dulaimi, "The dependence of the energy density states on the substitution of chemical elements in the $\text{Se}_6\text{Te}_{4-x}\text{Sb}_x$ thin film," Chalcogenide Letters, vol. 19, no. 4, pp. 301–308, 2022.
21. G. Che, Y. Du, F. Wu, Y. Yang, C. Dong, and Z. Zhao, "Effect of quenching on the superconductivity and oxygen content of $\text{Bi}(\text{pb})\text{-}2223$ phase," Solid State Communications, vol. 89, no. 11, pp. 903-906, 1994, doi: 10.1016/0038-1098(94)90347-6.
22. K. A. Jasim and L. A. Mohammed, "The partial substitution of copper with nickel oxide on the Structural and electrical properties of $\text{HgBa}_2\text{Ca}_2\text{Cu}_3\text{xNi}_x\text{O}_{8+\delta}$ superconducting compound," Journal of Physics: Conference Series, vol. 1003, p. 012071, 2018.
23. M. Collins, "Research: An introduction to principles, methods and practice," Evaluation and Program Planning, vol. 23, no. 4, pp. 472-473, 2000, doi: 10.1016/s0149-7189(00)00038-0.

24. W. Tian, H. M. Shao, J. S. Zhu, and Y. N. Wang, "Physica Status Solidi," *Physica Status Solidi (a)*, vol. 203, no. 11, 2006, doi: 10.1002/pssa.v203:11.
25. K. A. Jasim and S. A. Makki, "Comparison study of transition temperature between the superconducting compounds $Tl_{0.9}Pb_{0.1}Ba_2Ca_2Cu_3O_9$, $Tl_{0.9}Sb_{0.1}Ba_2Ca_2Cu_3O_{9-\delta}$ and $Tl_{0.9}Cr_{0.1}Ba_2Ca_2Cu_3O_{9-\delta}$," *Physics Procedia*, vol. 55, pp. 336–341, 2014.
26. L. A. Mohammed and K. A. Jasim, "Improvement the superconducting properties of $TlBa_2Ca_2Cu_3xNi_xO_{9-\delta}$ superconducting compound by partial substitution of copper with nickel oxide," *Energy Procedia*, vol. 157, pp. 135-142, 2019, doi: 10.1016/j.egypro.2018.11.173.
27. K. A. Jasim, T. J. Alwan, K. H. Mahdi, H. L. Mansour, "The effect of neutron irradiation on the properties of $Tl_{0.6}Pb_{0.3}Cd_{0.1}Ba_2Ca_2Cu_3O_{9-\delta}$ superconductors," *Turkish Journal of Physics*, vol. 37, no. 2, pp. 237–241, 2013, doi: 10.3906/fiz-1203-16.
28. K. A. Jasim and T. J. Alwan, "Effect of oxygen treatment on the structural and electrical properties of $Tl_{0.85}Cd_{0.15}Sr_2CuO_5-\delta$, $Tl_{0.85}Cd_{0.15}Sr_2Ca_2Cu_2O_7-\delta$ and $Tl_{0.85}Cd_{0.15}Sr_2Ca_2Cu_3O_{9-\delta}$ superconductors," *Journal of Superconductivity and Novel MZn netism*, vol. 30, no. 12, pp. 3451-3457, 2017.
29. B. B. Kadhim, I. H. Khaleel, B. H. Hussein, B. K. H. Al-Maiyaly, S. H. Mahdi, "Effect of gamma irradiation on the $TlBa_2Ca_2Cu_3O_{9-\delta}$ superconducting properties," *AIP Conference Proceedings*, vol. 1968, p. 030054, 2018.